# Flow structure in compound open-channel flows in the presence of transverse currents

*Sébastien* Proust[1,*], and *Vladimir* Nikora[2]

[1]Irstea, UR RiverLy, centre de Lyon-Villeurbanne, 5 rue de la Doua CS 20244, 69625 Villeurbanne, France
[2]School of Engineering, University of Aberdeen, Fraser Noble Building, Kings College, Aberdeen, United Kingdom

**Abstract.** The structure of free-surface flows is experimentally investigated in a laboratory flume with a compound cross-section consisting of a central main channel (MC) and two adjacent floodplains (FPs). The study focuses on the effects of transverse currents on: (i) mixing layers and quasi-two-dimensional coherent structures at the interfaces between MC and FPs; (ii) secondary currents developing across the channel; and (iii) large and very-large-scale motions that were recently observed in non-compound open channel flows. Transverse currents represent spanwise depth- and time-averaged flow from MC to FPs or vice versa. The study is based on one-point and two-point ADV measurements. Streamwise non-uniform flows are generated by imposing an imbalance in the discharge distribution between MC and FPs at the flume entrance, keeping the total flow rate the same for all scenarios. It is shown that even small transverse currents can be very effective in flow modification, as they can significantly displace the mixing layer, shear-layer turbulence, and coherent structures towards MC or FP, depending on the current direction. They can also alter the distribution and strength of the secondary currents. The interactions of quasi-two-dimensional coherent structures, very-large-scale motions, and secondary currents at different conditions are also part of this study.

## 1. Introduction

Overflowing rivers may give rise to streamwise non-uniform flows in compound channels, which consist of the main river channel (MC) and one or two floodplains (FPs). Flow non-uniformity can be caused by longitudinal changes in the topography or land use of FPs, by backwater surface profiles, or by an unbalanced flow distribution between MC and FPs at the upstream boundary of a river reach. Flow non-uniformity is associated with longitudinal changes in flow depth, often accompanied by transverse currents. These currents represent transverse depth-averaged and time-averaged flows from MC to FPs or vice versa, quantified by the depth-averaged transverse velocity $U_{yd}$.

We present here a part of a laboratory study that focuses on the effects of transverse currents on the flow structure in compound open-channel flows, namely on: (i) mixing

---

* Corresponding author: sebastien.proust@irstea.fr

layers and quasi-two-dimensional Kelvin-Helmholtz type coherent structures (CSs) that form at the interfaces between the MC and the two FPs; (ii) secondary current cells developing across the channel; and (iii) large and very-large-scale motions that were recently observed by [1] in non-compound rough-bed open channel flows. The present paper will only focus on (i) and (ii). Flow non-uniformity and associated transverse currents are generated in the study by creating an imbalance in the upstream discharge distribution between MC and FPs in a prismatic compound open-channel (see *e.g.,* [2-3]).

The paper outlines experimental set up and flow scenarios first, followed by the presentation of the results related to mixing layer parameters, large-scale 2D CSs, and secondary currents.

## 2. Experimental set-up and flow conditions

### 2.1. Flume and velocity measurements



**Fig. 1.** Compound open-channel flume (18m × 3m), Irstea Lyon-Villeurbanne, France.

The experiments were performed in an 18 m long and 3 m wide compound channel flume that is located in the Hydraulics and Hydro-morphology Laboratory of Irstea, Lyon-Villeurbanne, France. The flume bottom slope is $1.1 \times 10^{-3}$. The compound cross-section is composed of a 1 m wide rectangular glassed-bed MC and of two 1 m wide lateral rough-surface FPs, which are covered with dense plastic grass (5 mm high rigid blades). The vertical distance from the MC bottom to the blades top is 117 mm, defining the bankfull stage in the MC. A Cartesian coordinate system is used in which $x$, $y$, and $z$ axes are aligned with the longitudinal (along the flume), transverse, and vertical (normal to the flume bottom) directions. The system origin is defined as: $x = 0$ at the outlet of the three inlet tanks (one per sub-section, *i.e.* MC, right-hand and left-hand FPs); $y = 0$ at the side-wall of the right-hand FP; and $z = 0$ at the MC bottom.

The study is based on one-point and two-point Acoustic Doppler Velocimetry measurements. We have used two 3D Nortek Vectrino+ Acoustic Doppler Velocimeters (ADVs), with a side looking probe (sampling volume 5 cm away from the probe). The sampling volume of an ADV can be approximated as a cylinder 6 mm in diameter and 7 mm long. At each measuring point, the three velocity components ($u$, $v$, $w$) were recorded at 100 Hz for 300 s. The ADV data were despiked using the phase-space thresholding technique of [4].
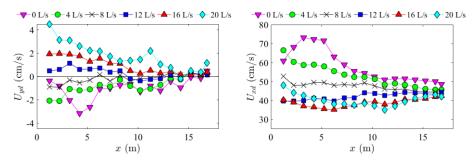
## 2.2. Flow conditions

The flow conditions selected for experiments are given in Table 1. The experiments started with stream-wise uniform flow conditions in the absence of the depth-averaged and time-averaged transverse currents, with a constant flow depth in the longitudinal direction and with constant discharges in each FP ($Q_f$ = 8 L/s) and in the MC ($Q_m$ = 98 L/s). Streamwise non-uniform flows are then generated by imposing an imbalance in the discharge distribution between MC and FPs at the flume entrance, keeping the total flow rate ($Q$ = 114 L/s) the same as for the uniform flow setup. Five unbalanced inflow conditions have been tested, with inflow $Q_f(x = 0)$ of 0, 4, 12, 16 and 20 L/s at each FP. The created non-uniform flows are associated with longitudinal changes in the flow depth and with the transverse currents.

**Table 1.** Flow conditions of test cases: inflow in each of the two FPs $Q_f(x = 0)$ and in the MC $Q_m(x = 0)$, the total flow rate being $Q$ = 114 L/s; ranges of longitudinal variations of the FP flow depth $D_f$ and stream-wise mean velocity outside the mixing layer on the high-speed flow side ($U_{x2}$) and low-speed flow side ($U_{x1}$) (between $x$ = 2.4 m and 16.4 m).

| Cases | $Q_f(x = 0)$ (L/s) | $Qm(x = 0)$ (L/s) | $D_f$ (cm) | $U_{x1}$ (cm/s) | $U_{x2}$ (cm/s) |
|-------|-----|-----|-----|-----|-----|
| 0 L/s | 0 | 114 | 18.6 – 31.1 | 0 – 21.2 | 87.9 – 84.1 |
| 4 L/s | 4 | 106 | 25.2 – 31.0 | 13.8 – 22.0 | 74.7 – 82.9 |
| 8 L/s | 8 | 98 | 30.8 – 30.3 | 25.6 – 24.7 | 67.2 – 83.7 |
| 12 L/s | 12 | 90 | 35.2 – 31.1 | 33.7 – 22.2 | 64.5 – 81.7 |
| 16 L/s | 16 | 82 | 36.4 – 30.4 | 38.9 – 24.2 | 58.9 – 79.5 |
| 20 L/s | 20 | 74 | 38.6 – 31.5 | 44.6 – 23.8 | 53.4 – 78.9 |

# 3. Results

## 3.1. Transverse currents



**Fig. 2.** Time-averaged and depth-averaged transverse and stream-wise velocities, $U_{yd}$ and $U_{xd}$, respectively, along the right-hand interface MC/FP.

The depth- and time-averaged flow velocities at the MC/FP interface is shown in Figure 2. The peak values of the ratio between transverse and stream-wise velocity components, $U_{yd} / U_{xd}$, ranges from −4% to 9%, highlighting the weakness of transverse currents with

respect to the main flow in stream-wise direction. However, the transverse velocity $U_{yd}$ is of the order of magnitude of the depth-averaged root mean square of transverse velocity fluctuation, $u'_y$ (in the range from 2 cm/s to 8 cm/s, not shown here). We can thus expect a strong interaction between transverse currents and shear layer turbulence.

Regarding the case of 8 L/s (Table 1), which is uniform in the stream-wise direction (*i.e.*, no change in depth along the flow; see $D_f$-values in Table 1), it is interesting to note that the interfacial velocity $U_{xd}$ is evolving within the whole measuring domain, as a reflection of the mixing layer development. The negative $U_{yd}$-values observed along the first half of the flume (Figure 2) may be due to: (i) a small underestimation of the FP inflow required for streamwise uniformity; or/and (ii) the uniform distribution across the channel of the stream-wise mean velocity at the outlet of each of the three inlet tanks ($x = 0$). Both inevitably lead to a small mass transfer from MC to FP.
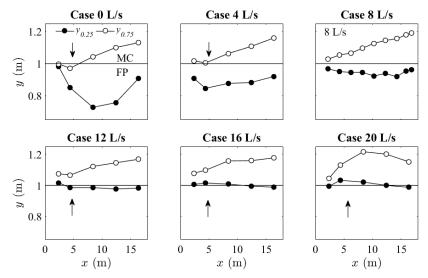
### 3.2. Mixing layer width

The mixing layer width based on mean flow consideration is shown in Figure 3. The definition of [5] is used, *i.e.*:

$$\delta = 2 \, (y_{75\%} - y_{25\%}) \tag{1}$$

where $U_x(y_{25\%}) = U_{x1} + 0.25(U_{x2} - U_{x1})$ and $U_x(y_{75\%}) = U_{x1} + 0.75(U_{x2} - U_{x1})$. Here, $U_{x1}$ is the stream-wise velocity averaged across the plateau region over the FP, and $U_{x2}$ is the peak velocity in the MC.

Let us consider the mixing layer width for the case of 8 L/s (uniform flow) as the reference width. In the presence of the transverse currents, the mixing layer is strongly laterally displaced in the direction of the current. For cases of 12, 16 and 20 L/s, three-quarters of the mixing layer are located in the MC along the whole flume, even though transverse velocity $U_{yd}$ is very small in the second part of the flume (Figure 2). With transverse currents in the opposite direction (cases 0 and 4 L/s), three-quarters of $\delta$ are located over the FP, but only in the upstream part of the flume until $x = 4.4$ m. This shows a significant asymmetry in the relaxation towards the reference width, with a faster relaxation when currents are directed towards the FP.
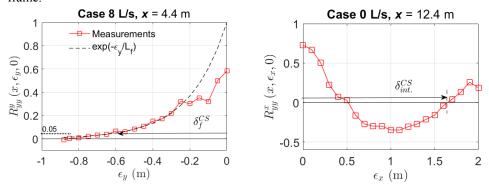


**Fig. 3.** Half the mixing layer width, $\delta / 2$, according to [5], with $\delta = 2 \, (y_{0.75} - y_{0.25})$. Arrow indicates the direction of transverse currents.

### 3.3. Coherent structure length scales

To investigate the development of CSs along the flume, space-time correlations of velocity fluctuations were used (based on two-point velocity measurements). Figure 4 shows spatial autocorrelation function (with zero time lag) of the transverse velocity fluctuation, $u_y'$, across the FP (left plot), and along the MC/right-FP interface (right plot). The space-time correlation function is defined as:

$$R_{ij}^k(x_k, \varepsilon_k, \tau) = \frac{\overline{u_i'(x_k, t)u_j'(x_k + \varepsilon_k, t + \tau)}}{\left(\overline{u_i'^2(x_k)} \cdot \overline{u_j'^2(x_k + \varepsilon_k)}\right)^{0.5}} \tag{2}$$

where $u_i'$ is velocity fluctuation, $\varepsilon_k$ is spatial lag in the $k$-direction, and $\tau$ is time lag.

In general, $R_{ij}^k(x_k, \varepsilon_k, \tau)$ in Eq. (2) depends on the location of a reference point where a measurement probe is fixed with another probe moving away point by point. Here, the reference point is always located at the MC/FP interface. The second probe is moving laterally in the MC or over the FP, or longitudinally along the interface downstream the flume.



**Fig. 4.** Definition of the experimental length scales of the CSs: $\delta_{int}^{CS}$ is the longitudinal length scale along the interface MC/FP; $\delta_f^{CS}$ is the transverse length scale in the right-hand FP; and $\delta_m^{CS}$ is the transverse length scale in the MC (not shown).

To reduce potential uncertainties due to the shape of the correlation functions and limited maximum lag, we do not use the integral scales and instead we define the characteristic scales of the CSs as spatial lags corresponding to a particular correlation level (*e.g.*, [6-7]). The transverse characteristic scale $\delta_f^{CS}$ corresponds to the transverse distance from the interface to the $y$-value where $R_{yy}^y = 0.05$. Note that this distance, in isotropic homogeneous turbulence, is of the order of $3L_f$ (Eq. 3) $- L_f$ defining the integral length scale $-$ if the autocorrelation function is approximated by $\exp(-y/L_y)$, *i.e.*:
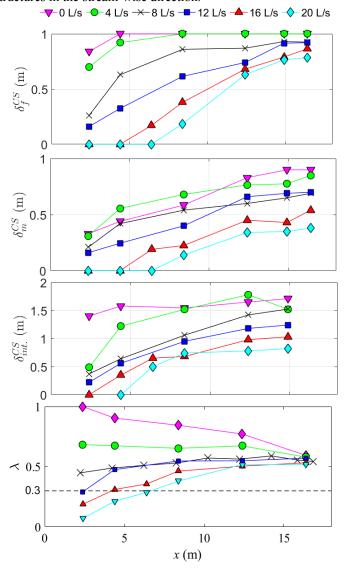
$$L_f = \int_{-\infty}^{0} R_{yy}^y \, dy \tag{3}$$

This approximation was tested (Figure 4 left) and fairly match the experimental data for the case of 8 L/s at $x = 4.4$ m within the area where the two probes do not have an influence on each other. The same definition was used for $\delta_m^{CS}$ in the MC. Note also that the correlation level of 0.05 also represents a level below which the correlation is not distinguishable from zero.

Relying on [8-9], who have shown the strong asymmetry of the compound channel mixing layer compared to the free mixing layer, the length scales of the CSs on either side

of the MC/FP interface will be distinguished. The characteristic width of the CS is defined as a sum of MC-hand and FP-hand scales, *i.e.*:

$$\delta^{CS} = \delta_m{}^{CS} + \delta_f{}^{CS} \qquad (4)$$

The stream-wise scale, $\delta_{int}{}^{CS}$, corresponds to the longitudinal distance between the upstream fixed probe and the downstream moving probe when $R_{yy}{}^y$ crosses zero for the second time (Figure 4 right). This scale corresponds, approximately, to the ¾ of the spacing between the structures in the stream-wise direction.



**Fig. 5.** Measurements of transverse length scales in the MC and FP, $\delta_m{}^{CS}$ and $\delta_f{}^{CS}$, respectively. Longitudinal length scale along the interface, $\delta_{int}{}^{CS}$; dimensionless shear $\lambda = (U_{x2} - U_{x1}) / (U_{x1} + U_{x2})$.

Figure 5 shows three experimental lengths scales of CSs. First main tendency to note is an increase of the CSs size in the transverse direction (both in the MC and FP) and in the longitudinal direction, when going downstream. Second, CSs are observed along the whole

measuring domain for the cases of 0, 4, 8, and 12 L/s, but not for the cases of 16 and 20 L/s (Table 1). For these two cases, CSs are absent in the very upstream part of the flume at $x = 2.4$ m. Yet, the destabilizing shear $U_{x2} - U_{x1}$ (*e.g.,* [10]) responsible for the Kelvin-Helmholtz instabilities is not negligible (see the values in Table 1 at $x = 2.4$ m). In fact, the existence of CSs is found to be related to the local value of dimensionless shear $\lambda$ (Figure 5 bottom), defined as:

$$\lambda = (U_{x2} - U_{x1}) / (U_{x2} + U_{x1}) \tag{5}$$

This result, based on two-point measurements, is a confirmation of the one point measurements of [11], who have investigated 25 flow cases in two different flumes with three levels of vertical flow confinement. A dimensionless shear parameter $\lambda$ higher than 0.3 was found to be a necessary condition for the development of Kelvin-Helmholtz type large scale CSs, irrespective of flow confinement, *i.e.* of the influence of flow depth and bed-induced turbulence. In figure 5, no CS can be observed if $\lambda < 0.3$. When $\lambda \geq 0.3$, CSs start developing along the interface before diffusing laterally in the MC and the FP (see $\delta_{int}^{CS}$, $\delta_m^{CS}$, $\delta_f^{CS}$ for cases 16 and 20 L/s). As stated by [8], the vertical interface, which is the location of the mean velocity profile inflection point, is the core of the CSs formation.
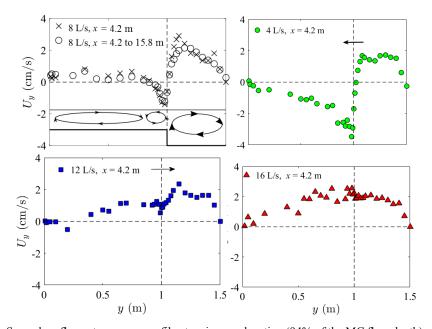
## 3.4. Secondary flows



**Fig. 6.** Secondary flows: transverse profile at a given z-elevation (94% of the MC flow depth).

Lateral near-surface profiles of the transverse mean velocity $U_y$ at the distance from the bed of 94% of the MC flow depth are shown in Figure 6. For the case of 8 L/s, a longitudinally averaged value $< U_y >_x$ between $x = 4.2$ m and 15.8 m is also displayed.

For uniform flow case of 8 L/s, both $U_y$ and $<U_y>_x$-distributions suggest the existence of three different secondary current cells in the near-surface region, as previously observed by [12] in a compound channel with the rough-surface FPs. With transverse currents towards the MC (cases 12 and 16 L/s), these preliminary results show that the secondary current cell near the interface on the FP side might vanish, which might lead to a single cell across the

compound channel above the bankfull stage in the MC. With the transverse currents towards the FP, this interfacial cell might also vanish, giving rise to a single cell over the FP rotating in the opposite direction compared to the cell in the MC. This has to be confirmed by additional measurements across the FP at various elevations, as the previous result might also be related to the transverse net mass transfer.

## 4. Conclusion

The reported laboratory study has shown that even small transverse currents (4 to 9% of the stream-wise mean flow) can be very effective in flow modification, as they can significantly displace the turbulent mixing layer, depending on the current direction. They can also alter the pattern, distribution and strength of the secondary currents. The spatial autocorrelations of transverse velocity, based on two-point velocity measurements, have confirmed the existence of a threshold value of the dimensionless shear $\lambda = (U_{x2} - U_{x1}) / (U_{x1} + U_{x2})$, around 0.3, for the development of the Kelvin-Helmholtz instabilities. As the $\lambda$-parameter is a purely two-dimensional parameter, new experiments could be undertaken to evaluate the role played by this parameter in other flow configurations such as shallow mixing layers in non-compound geometries or mixing layers at river confluences.

## References

1. S. M. Cameron, V. I. Nikora, M. T. Stewart, J. Fluid Mech., **814**, 416-429 (2017)

2. D. Bousmar, N. Rivière, S. Proust, A. Paquier, R. Morel, Y. Zech, J. Hydraul. Eng., ASCE, **131**, 5, 408-412 (2005)

3. S. Proust, J. N. Fernandes, Y. Peltier, J. B. Leal, N. Rivière, A. H. Cardoso, J. Hydraul. Res., **51**, 6, 656-667 (2013)

4. D. G., Goring, V. Nikora, J. Hydraul. Eng. **128**, 1, 117-126 (2002)

5. B. C.Van Prooijen, J. A. Battjes, W. S. J. Uijttewaal, J. Hydraul. Eng., **131**, 3, 175-183 (2005)

6. P. L. O'Neill, D. Nicolaides, D. Honnery, J. Soria, *15th Australasian Fluid Mech. Conf.*, p. 4, The University of Sydney, Australia (2004)

7. J. M. McDonough, Introductory lectures on turbulence. Physics, Mathematics and Modeling, Departments of Mechanical Engineering and Mathematics, University of Kentucky (2007)

8. V. Dupuis, S. Proust, C. Berni, A. Paquier, Exp. Fluids, **58**, 30, 1-18 (2017a)

9. V. Dupuis, S. Proust, C. Berni, A. Paquier, Environ. Fluid Mech., **17**, 5, 903-928 (2017b)

10. P. Huerre, M. Rossi, Hydrodynamic instabilities in open flows, in *Hydrodynamics and Nonlinear Instabilities* edited by C. Godrèche and P. Manneville, pp. 81-294, Cambridge University Press (1998)

11. S. Proust, J. N. Fernandes, J. B. Leal, N. Rivière, Y. Peltier, Water Resour. Res., **53**, 4, 3387–3406 (2017)

12. A. Tominaga, I. Nezu, J. Hydraul. Eng., **117**, 1, 21-41 (1991)